

Eckart streaming with nonlinear high-order harmonics: An example at gigahertz

Shiyu Li


*State Key Laboratory of Ocean Engineering, School of Ocean and Civil Engineering,
Shanghai Jiao Tong University, Shanghai 200240, China*

Weiwei Cui

*State Key Laboratory of Precision Measuring Technology and Instruments,
Tianjin University, Tianjin 300072, China*

Thierry Baasch

Department of Biomedical Engineering, Lund University, Lund, Sweden

Bin Wang and Zhixiong Gong *

*State Key Laboratory of Ocean Engineering, School of Ocean and Civil Engineering,
Shanghai Jiao Tong University, Shanghai 200240, China
and Key Laboratory of Marine Intelligent Equipment and System, Ministry of Education, China*



(Received 1 March 2024; accepted 19 July 2024; published 8 August 2024)

Acoustic streaming shows great potential in applications such as bubble dynamics, cell aggregation, and nanosized particle isolation in the biomedical and drug industries. As the acoustic shock distance decreases with the increase of incident frequency, the nonlinear propagation effect will play a role in acoustic streaming, e.g., Eckart (bulk) streaming at a few gigahertz. However, the theory of source terms of bulk streaming is still missing at this stage when high-order acoustic harmonics play a role. In this paper, we derive the source term including the contribution of high-order harmonics. The streaming-induced hydrodynamic flow is assumed to be incompressible and no shock wave occurs during the nonlinear acoustic propagation as restricted by the traditional Goldberg number $\Gamma < 1$ or $\Gamma \approx 1$, which indicates the importance of nonlinearity relative to dissipation. The derived force terms allow evaluating bulk streaming with high-order harmonics at gigahertz and provide an exact expression compared to the existing empirical formulas. Numerical results show that the contribution of higher-order harmonics increases the streaming flow velocity by more than 20%. Our approach clearly demonstrates the errors inherent in the expression introduced by Nyborg which should be avoided in numerical computations as it includes part of the acoustic radiation force that does not lead to acoustic streaming.

DOI: [10.1103/PhysRevFluids.9.084201](https://doi.org/10.1103/PhysRevFluids.9.084201)

I. INTRODUCTION

Gigahertz acoustics have recently been used in experiments for nanoparticle trapping, enrichment, and separation based on the acoustic streaming effect [1–3]. Acoustic manipulation in the gigahertz range has potential applications including nanosized biosensors [2], nanoliter microreactors [4], and microfluid jet producers [5]. However, the study of gigahertz streaming is just at

*Contact author: zhixiong.gong@sjtu.edu.cn; <https://en.naoce.sjtu.edu.cn/teachers/GongZhixiong.html>

the beginning due to the challenges of fabrication techniques of ultrahigh frequency resonators [6] and the huge computational costs with direct numerical simulations at such small wavelengths, especially in three dimensions [7]. For a typical gigahertz tweezer, the wavelength is $1.5 \mu\text{m}$ at the frequency of 1 GHz in water, which is much smaller than typical microchannel sizes, e.g., a few tens or hundreds of micrometers. In addition, it is easy to induce nonlinear propagation at gigahertz since the shock formation distance (hereafter referred to as shock distance) depends on the working frequency and the large vibration velocity on the transducer surface [8,9]. These make the theoretical and experimental studies of gigahertz acoustic tweezers more challenging compared to that in the frequency regime of megahertz.

The sound waves are produced based on mechanical vibration and are coupled into the fluid medium for microfluidic applications. The highest efficiency of energy conversion from electrical to mechanical energies typically occurs at the mechanical resonance, which depends on the desired acoustic wavelength (or driving frequency). The wavelengths of typical gigahertz transducers in the coupling medium range from around 100 nm to a few micrometers, leading to the difficulties of device fabrication. Typical piezoelectric transducers (PZT) use the vibration of planar sources to produce acoustics with a frequency regime of 1–10 MHz in the field of acoustofluidics. However, it is a challenge to fabricate PZT at the thickness of nanometers for the frequency at gigahertz since the resonance depends on the selected vibration mode depending on the piezo thickness. Considering interdigitated transducers [10] at gigahertz, the distances between electrode fingers are too small to fabricate with the commonly used fabrication process and cannot withstand high power [6]. This is partly solved with the successful fabrication of the high-tone bulk acoustic resonators on four substrates with very high Q factor (up to 48 000) at 1 GHz [11]. Then, Cui *et al.* [1] combined the fabrication of the film bulk acoustic wave resonator technique with micro/nanofluidics and developed the field of gigahertz acoustofluidics.

Compared with the recent development of fabrication techniques and experimental demonstrations of gigahertz acoustical tweezers, the theories of acoustic bulk streaming at such high frequencies are not well studied. For most of the published experimental works at gigahertz, empirical expressions of the source term of acoustic streaming are used in the numerical simulations, and no one seems to verify the streaming flow velocities between the simulation and experiment results [2,3]. This is generally due to two challenges: (i) There is no available source term for gigahertz bulk streaming with the consideration of nonlinear acoustic propagation. (ii) The computational cost of the real experiment configuration is huge because of the small wavelength at the scale of a few micrometers. Indeed, it is easy to understand that the streaming-induced flow patterns are similar in the confined microchannels because of the mass conservation of the steady flow. Since the seminal works of Eckart [12], Nyborg [13,14], and Lighthill [15], the systematic theories of the bulk (Eckart) streaming are built and developed. A good historical perspective of bulk acoustic streaming can be found in Ref. [16]. It should be noteworthy that Nyborg derived an expression of the source term of bulk streaming to solve the Stokes equation for the hydrodynamic flow velocity [13,14] which is widely used in the research community of this field. However, as pointed out by Lighthill, the source term by Nyborg contains a gradient term that makes a contribution to the acoustic radiation pressure instead of streaming [15,16]. The source term of acoustic streaming was recast recently by Riaud *et al.* specifying the sole source of bulk streaming without the gradient of acoustic Lagrangian [17]. In their work, they consider the bulk streaming inside sessile droplets of size 1 mm under the activation of surface acoustic waves at a frequency of around 20 MHz neglecting the nonlinear propagation since the Goldberg number [defined in Eq. (1) below] is much smaller than 1 and the droplet size is much smaller than the shock distance. Hence, the source term is limited to linear propagation when there are no high-order acoustic harmonics. However, the nonlinear effect of acoustic propagation cannot be neglected in the frequency regime of gigahertz since the viscous dissipation is remarkable and the dimensionless Goldberg number is comparable to the unit. This is the case for the recent experimental works at gigahertz [1].

In this work, we revisit the source term of bulk acoustic streaming with two assumptions: (i) acoustics are rotational and (ii) the streaming-induced steady hydrodynamic flow is incompressible.

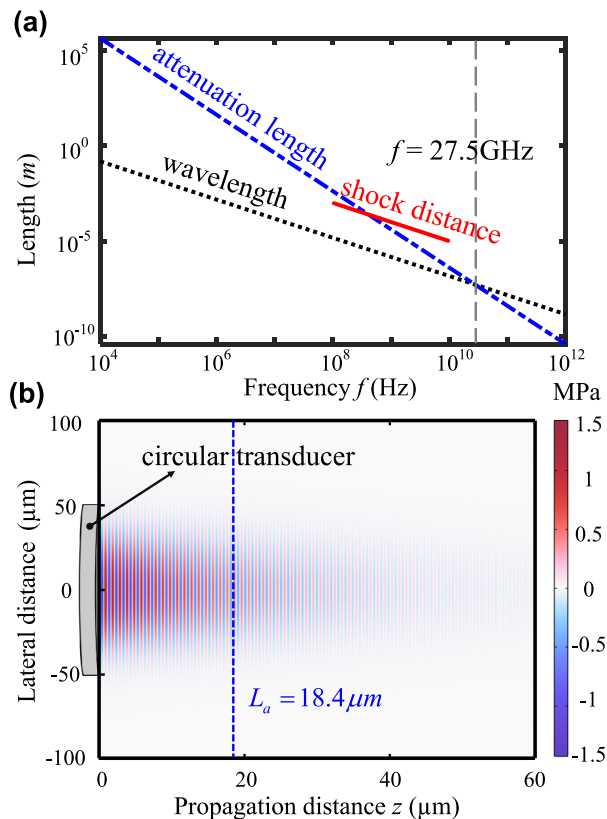


FIG. 1. (a) The wavelength, acoustic attenuation length, and shock distance versus the incident frequency from 0.01 MHz to 1000 GHz (both axes are in logarithmic coordinates). $B/A = 5.1$ is taken from Ref. [18] for water. The vibration velocity to estimate the shock distance is $U_{ac} = 1$ m/s based on previous experimental results from 0.1 to 10 GHz. The attenuation length L_a is equal to the incident wavelength $\lambda = 0.055$ μm at $f \approx 27.5$ GHz (see the gray dashed line). (b) For a special case at frequency $f = 1.5$ GHz, the wavelength is $\lambda = 1$ μm , the attenuation length is $L_a = 18.4$ μm , and the shock distance is $L_s = 67.2$ μm . The pressure field in the propagation plane with a circular transducer at $f = 1.5$ GHz is shown. The pressure is computed using the “thermoacoustic” interface in COMSOL Multiphysics 6.0 [19] with the detailed governing equations and boundary conditions given in Sec. III C.

Only weakly nonlinear effects with harmonic waves are taken into consideration and the shock wave is outside of scope since it will make the second assumption fail. Both theoretical and numerical examples are proposed to illustrate the issue of Nyborg’s expression which should be avoided as shown in Sec. III. More importantly, based on the peculiar characteristics of bulk streaming at gigahertz, the nonlinear effect of acoustic propagation will be considered and a theoretical source term for this situation is provided in terms of pressure fields of different orders of harmonics. This work provides a theoretical basis for steady streaming at gigahertz with high-order harmonics.

II. CHARACTERISTIC LENGTHS IN THE FREQUENCY REGIME NEAR 1 GHZ

Compared with the general frequencies in the medical ultrasonic regime (e.g., 1–10 MHz), there are two different characteristics in the regime near 1 GHz as shown in Fig. 1(a): (i) The attenuation length $L_a = 2\rho_0 c_0^3 / [\omega^2 \mu_s b]$ is just one order of magnitude as the wavelength at the typical megahertz regime, and the acoustic Reynolds number is $\text{Re}_{ac} = L_a / \lambda \gg 1$ [17]. ρ_0

TABLE I. Physical parameters. The fluid medium in this work is water. f is the incident frequency. Another nonlinear parameter is defined as $\beta = 1 + B/2A$. U_{ac} is the magnitude of the acoustic velocity perturbation at the transducer surface. Note that a factor of 2 is missing in the definition of L_a in Refs. [16,17].

Symbol	Physical parameter	Value
ρ_0	Static density	1000 kg/m ³
c_0	Acoustic velocity	1500 m/s
ω	Angular frequency	$2\pi f$
μ_s	Dynamic viscosity	1.002×10^{-3} Pa s
ν	Kinematic viscosity	μ_s/ρ_0
μ_b	Bulk viscosity	2.8×10^{-3} Pa s
b	Defined coefficients	$4/3 + \mu_b/\mu_s$
Γ	Goldberg number	L_a/L_s
L_a	Acoustic attenuation length	$2\rho_0 c_0^3/[\omega^2 \mu_s b]$
L_s	Shock distance	$c_0^2/[\omega \beta U_{ac}]$ [16]
Re_{ac}	Acoustic Reynolds number	L_a/λ
Re_{hd}	Hydrodynamic Reynolds number	$\rho_0 \mathbf{v}_2 L_c / \mu_s$
δ	Boundary layer thickness	$\sqrt{2\nu/\omega}$
L_c	Microchannel height	60 μm

is the static mass density of the propagation medium, c_0 is the sound speed, ω is the angular frequency, and $b = 4/3 + \mu_b/\mu_s$ is the defined coefficient related to dynamic (μ_s) and bulk (μ_b) viscosities for convenience. The related physical parameters and values for the medium of water are listed in Table I. At $f = 1.5$ GHz in water, the wavelength is $\lambda = 1$ μm and the attenuation length is $L_a = 18.4$ μm [see Fig. 1(b) for the pressure distribution]. While at $f = 1.5$ MHz in water, it has $\lambda = 1$ mm and $L_a = 1.84 \times 10^4$ mm. (ii) The attenuation length is comparable with the shock distance $L_s = c_0^2/[\omega \beta U_{ac}]$ at the typical vibration velocity of the transducer working at gigahertz (e.g., $U_{ac} = 1$ m/s). $\beta = 1 + B/[2A]$ is the nonlinear parameter with two nonlinear acoustic coefficients A and B . $A = \rho_0 c_0^2$ and $B = \rho_0^2 (\partial^2 p / \partial \rho^2)_s$ are the first- and second-order coefficients in the Taylor expansion of pressure and density associated with the material, and the subscript s represents an isentropic process [8,16,17]. At $f = 27.5$ GHz as marked with the gray dashed line in Fig. 1(a), the attenuation length equals the wavelength, i.e., $L_a = \lambda = 0.055$ μm . That is to say, most of the energy from the transducer will dissipate in the propagation distance of one wavelength. In this work, only low gigahertz transducers for acoustic steaming will be studied and they have been used most in recent microfluidics experiments in the regime of gigahertz. In fact, the shock distance describes the nonlinearity of the acoustic propagation and the attenuation length is an indicator of the wave dissipation in the medium. Here, the Goldberg number Γ is introduced to provide a dimensionless measure of the importance of nonlinearity relative to dissipation with the definition

$$\Gamma = \frac{L_a}{L_s} = \frac{2\rho_0 c_0 \beta U_{ac}}{\omega \mu_s b}. \quad (1)$$

Note that the attenuation length L_a is independent of the activation velocity U_{ac} , while the shock distance L_s has a linear relation with it. In general, there are no high-order harmonics during the acoustic propagation with $\Gamma \ll 1$, which is the case in Ref. [17]. When Γ is around the unit, it is possible to induce the high-order harmonics which will be discussed in detail in Sec. IV. Note that the shock distance depends on the U_{ac} and for the case of $U_{ac} = 1$ m/s in Fig. 1(a), Γ equals 1 (i.e., $L_s = L_a$) at $f = 0.407$ GHz. However, the source term of bulk streaming with the consideration of high-order acoustic harmonics is not available and this will be solved in the present work.

III. REVISIT OF SOURCE TERM FOR BULK STREAMING

A. Source term of bulk streaming

Before studying the streaming effect with high-order harmonics, we need to revisit the source term of bulk streaming. By following the work in Ref. [17], we briefly recall the source term for the Eckart-type acoustic streaming with bulk waves. To derive the final formula of the streaming source term, we start with the constitutive equations including the conservation of mass and momentum in the fluid medium as

$$\frac{\partial \rho}{\partial t} + \nabla \cdot (\rho \mathbf{v}) = 0, \quad (2)$$

$$\frac{\partial \rho \mathbf{v}}{\partial t} + \nabla \cdot (\rho \mathbf{v} \otimes \mathbf{v}) = -\nabla p + \mu_s \Delta \mathbf{v} + \left(\frac{\mu_s}{3} + \mu_b \right) \nabla \nabla \cdot \mathbf{v}, \quad (3)$$

where ρ , \mathbf{v} , and p are the density, velocity vector, and pressure, respectively. t designates the time. The entropy (s) balance is ensured for the system with $ds = 0$ and the state equation is

$$p = p(\rho), \quad \text{with} \quad \left. \frac{\partial p}{\partial \rho} \right|_s = c_0^2. \quad (4)$$

The first-order equation of state is easily obtained by using the Taylor expansion with $p_1 = c_0^2 \rho_1$, where p_1 , ρ_1 are the first-order acoustic pressure and density. In general, compared with the viscous effect, the thermal effect is negligible because it is proportional to $\gamma - 1$ with γ the adiabatic index which is weak in liquids [17]. Since only small perturbation occurs with respect to the hydrostatic parameters, we can apply the perturbation method and hence decompose the physical field \mathcal{X} into three parts: hydrostatic \mathcal{X}_0 , acoustic \mathcal{X}_1 , and hydrodynamic \mathcal{X}_2 . Under the assumption with the perturbation method, we assume that $\mathcal{X}_0 \gg \mathcal{X}_1 \gg \mathcal{X}_2$. \mathcal{X} can be either a scalar or a vector. The time average of acoustic component \mathcal{X}_1 is equal to zero, written as $\langle \mathcal{X}_1 \rangle = 0$, while the hydrodynamic part \mathcal{X}_2 shows the nonlinear feature with its time average not equal to zero (i.e., $\langle \mathcal{X}_2 \rangle \neq 0$). Based on the above assumptions, we can expand the density ρ , pressure p , and velocity \mathbf{v} as follows:

$$\begin{aligned} \rho &= \rho_0 + \rho_1 + \rho_2, \\ p &= p_0 + p_1 + p_2, \\ \mathbf{v} &= \mathbf{0} + \mathbf{v}_1 + \mathbf{v}_2. \end{aligned} \quad (5)$$

Here the particle velocity \mathbf{v}_0 is zero since the fluid is assumed to be at rest in the absence of acoustic disturbance. By expanding the above mass and momentum conservation equations up to the first and second order with some algebraic operations (see details in Appendix A), the source term of acoustic streaming can be derived as

$$\mathbf{F}_s = - \left(\frac{4\mu_s}{3} + \mu_b \right) \left\langle \frac{\rho_1}{\rho_0} \Delta \mathbf{v}_1 \right\rangle, \quad (6)$$

where Δ is the Laplace operator with $\Delta \mathbf{v}_1 = \nabla^2 \mathbf{v}_1 = \nabla \cdot \nabla \mathbf{v}_1$. It is noteworthy that this formula excludes the contribution of the gradient of acoustic Lagrangian, which in fact will not induce the bulk acoustic streaming [15,17]. In addition, the gradient of acoustic Lagrangian is very large compared to the sole source term which can possibly result in large computational errors. The effect of the acoustic Lagrangian gradient has not been studied before and will be demonstrated numerically in this work (see Sec. III C).

As shown in Appendix B 1, by using the linear wave equation for monochromatic waves, the source term for acoustic streaming in Eq. (6) can be simplified as

$$\mathbf{F}_s = \left(\frac{4\mu_s}{3} + \mu_b \right) \frac{\omega^2}{\rho_0 c_0^4} \langle p_1 \mathbf{v}_1 \rangle, \quad (7)$$

which depends on the time-averaged acoustic intensity $\langle \mathbf{I} \rangle = \langle p_1 \mathbf{v}_1 \rangle$. It indicates that once the acoustic field is calculated, the source term to compute the steady fluid streaming (\mathbf{v}_2) is available to solve the Stokes equation derived in Eq. (A13):

$$-\nabla p_2^* + \mu_s \Delta \mathbf{v}_2 + \mathbf{F}_s = 0, \quad (8)$$

where p_2^* is the modified hydrodynamic pressure to remove the contribution of the average acoustic Lagrangian.

It is noteworthy that the classical source term for acoustic streaming simulation proposed by Nyborg [13,14] is widely used although it should be avoided (see the recent review in Ref. [16]):

$$\mathbf{F}_s^{Nb} = -\rho_0 \nabla \cdot \langle \mathbf{v}_1 \otimes \mathbf{v}_1 \rangle, \quad (9)$$

where $\langle \cdot \rangle$ is the time-average operator. Recent studies have shown that this expression is not completely related to acoustic streaming, which may cause large numerical errors, and the source term can be divided into two parts through mathematical derivation [16,17]. In the following, we propose an analytical example of a one-dimensional (1D) bulk standing wave and a numerical simulation of a two-dimensional (2D) traveling wave to show the difference between the streaming field induced by these two source terms, i.e., based on Eqs. (7) and (9) by Nyborg.

B. One-dimensional bulk standing-wave example

In this section, we take the ideal 1D bulk standing waves as an example to show the difference of the source terms from Nyborg and in Eq. (7). This simple case will easily show the contradiction of the two source terms for bulk streaming and can be well understood from the point of view of streaming physics. The acoustic velocity field and pressure field of the 1D plane standing waves can be expressed as the addition of two ideal counterpropagating plane waves:

$$\mathbf{v}_1 = 2v_{\text{am}} \sin(kz) \cos(\omega t) \mathbf{e}_z, \quad (10a)$$

$$p_1 = 2p_{\text{am}} \cos(kz) \sin(\omega t), \quad (10b)$$

where v_{am} and p_{am} are the amplitudes of the acoustic velocity and pressure, k is the wave number, and z is the space coordinate with the unit vector in the propagation direction \mathbf{e}_z . By substituting them into the Nyborg source term in Eq. (9), we can get the body force in the propagation direction as

$$\mathbf{F}_s^{Nb} = -2\rho_0 k v_{\text{am}}^2 \sin(2kz) \langle \cos(2\omega t) + 1 \rangle. \quad (11)$$

Obviously, the magnitude of the force \mathbf{F}_s^{Nb} does not vanish since the time dependence $\langle \cos(2\omega t) + 1 \rangle$ is not equal to 0. On the other hand, we can get the following different result if we use the source term in Eq. (7):

$$\mathbf{F}_s = \left(\frac{4\mu_s}{3} + \mu_b \right) \frac{\omega^2}{c_0^4 \rho_0} \langle p_1 \mathbf{v}_1 \rangle \propto \langle \sin(\omega t) \cos(\omega t) \rangle \quad (12)$$

which vanishes as 0 after the time-average procedure in one period. It is clear that these two results are contradictory. As observed from Eq. (7), the body force depends on the average acoustic intensity which is uniform in space for progressive ideal plane waves. Since the standing waves can be regarded as the addition of two counterpropagating plane waves, the body forces of each plane wave should have the same magnitude while in reversed directions, leading to the null of the total body force for the streaming effect. This physical explanation agrees with the results of Eq. (12). Indeed, the source term \mathbf{F}_s^{Nb} by Nyborg is not entirely related to the streaming, and it contains the gradient of acoustic Lagrangian which contributes to acoustic radiation pressure instead of streaming [15,17].

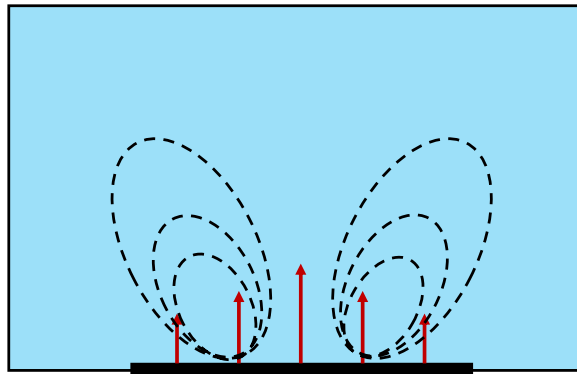


FIG. 2. The schematic of a 2D acoustic streaming by a planar transducer. The resonator (black area) excites gigahertz plane waves in the fluid (blue) and forms vortices (closed dashed lines) under the activation of body force (red arrow). In the acoustic simulation, the wall is set as the impedance boundary condition, and in the flow field simulation, the wall is set as the no-slip condition. Based on the conservation of fluid inside the cavity, the Eckart streaming always pushes the fluid up in the center and rolls back again from the two sides.

C. Numerical examples of 2D bulk streaming

Since the wavelength at gigahertz is in the order of nanometers or a few microns, it often needs small size steps in the computational domain based on the rules of thumb. Hence, the three-dimensional simulation of bulk streaming problems will suffer the challenge of a massive amount of numerical computation cost. To reduce the numerical burden, we build a 2D model as illustrated in Fig. 2, and this will not hinder our understanding of the acoustic streaming mechanism at this stage. The contradiction between the two streaming source terms has been revealed by the ideal 1D standing-wave model in Sec. III B. This section will further show the difference of hydrodynamic flow velocities through numerical simulations. In the following simulations, only the source terms are different [i.e., Eqs. (7) and (9)]. We use water as the propagation medium with the parameters listed in Table I. The excitation frequency is $f = 1.5$ GHz and the vibration velocity of the transducer with a radius $50 \mu\text{m}$ is $U_{ac} = 0.1$ m/s, leading to the Goldberg number $\Gamma = 0.027 \ll 1$. Under this condition, the source term of streaming in Eq. (7) is suitable without the consideration of nonlinear propagation. The boundary layer thickness (or viscous penetration depth) is $\delta = \sqrt{2\nu/\omega} = 22$ nm $\ll L_c = 60 \mu\text{m}$ with L_c the height of the microchannel. Meanwhile, the microchannel size is smaller than the shock distance $L_s = 67.2 \mu\text{m}$ so that the shock waves will not be accumulated and formed. Hence, the bulk streaming is dominant in the fluid domain and the Rayleigh boundary streaming can be negligible [20].

The numerical simulations of acoustic streaming in this paper are carried out by COMSOL Multiphysics 6.0 with the flowchart shown in Fig. 3(a). Since the “thermoacoustic” interface uses fewer approximations (and, of course, requires more computations) than the “pressure acoustics” interface in COMSOL, we use the thermoacoustic interface to calculate the first-order sound field for more accurate results. The governing equation of the thermal viscous sound field is as follows [21]:

$$\begin{aligned}
 \partial_t T_1 &= D_{th} \nabla^2 T_1 + \frac{\alpha T_0}{\rho_0 C_p} \partial_t p_1, \\
 \partial_t p_1 &= \frac{1}{\gamma \kappa} [\alpha \partial_t T_1 - \nabla \cdot \mathbf{v}_1], \\
 \rho_0 \partial_t \mathbf{v}_1 &= -\nabla p_1 + \mu_s \nabla^2 \mathbf{v}_1 + \left(\frac{\mu_s}{3} + \mu_b \right) \nabla (\nabla \cdot \mathbf{v}_1).
 \end{aligned} \tag{13}$$

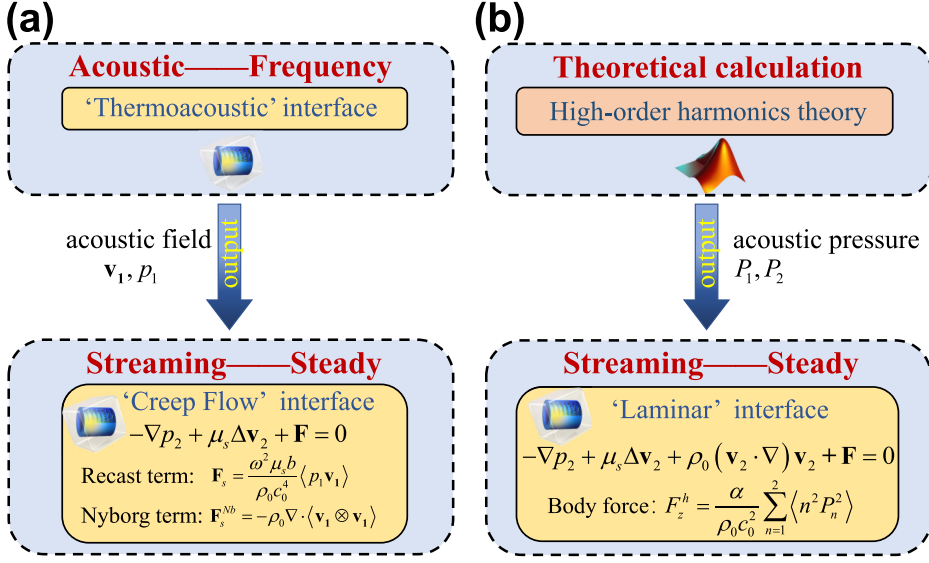


FIG. 3. The flowcharts of the simulation for bulk streaming (a) when the hydrodynamic Reynolds number is much smaller than 1; (b) when nonlinear propagation is considered.

Here, D_{th} is the thermal diffusivity, α is the isobaric thermal expansion coefficient, κ is the isentropic compressibility coefficient, and γ is the specific heat capacity ratio. Our research focuses on fluid motion within microchannels, therefore the effects of piezoelectric transducers are simulated with velocity boundary conditions:

$$\begin{aligned} u_{0x} &= 0, \\ u_{0y} &= U_{\text{ac}} e^{-R^2/a^2}. \end{aligned} \quad (14)$$

For PDMS walls, we use the impedance boundary to simplify the system:

$$n \cdot \nabla p_1 = -i \frac{\omega \rho_0}{\rho_i c_i} p_1, \quad (15)$$

where n is the normal vector, $\rho_i = 1070 \text{ kg/m}^3$ and $c_i = 1030 \text{ m/s}$ represent the density and sound velocity of PDMS, respectively, and i is an imaginary unit [22]. Under this boundary condition, the model assumes that all transmitted waves are absorbed by PDMS without reflecting back into the microchannel [23]. On the other hand, due to the severe attenuation of gigahertz sound waves (attenuation distance $L_a = 18.4 \text{ }\mu\text{m}$), the microchannel height is $H = 60 \text{ }\mu\text{m}$. Most sound waves are attenuated before coming into contact with the wall. Therefore, in this paper, we use impedance boundaries to simulate the influence of PDMS walls, which can better focus attention on the study of fluid motion in the channel. For the tangential velocity of the wall, we set it to $u_{\parallel} = 0$.

Then, the steady flow simulations are conducted based on the “creep flow” interface with the input of the source terms under the circumstance that the hydrodynamic Reynolds number is $\text{Re}_{\text{hd}} = 0.072 \ll 1$. All the walls were set with no-slip boundary conditions; that is, the Eulerian velocity field $u_2 = 0$. Indeed, the simulation with the “laminar” interface obtains the same streaming results as the creep flow interface case (not shown in the following for brevity).

In the 2D numerical simulations of bulk streaming, we set the volume forces in the propagation direction F_z and the lateral direction F_r with the flow velocities indicated by the colormap of the background and the directions indicated by the black arrows in Fig. 4. Because of the symmetry of the hydrodynamic flows in the microchannel, we show half of the simulation results and put them

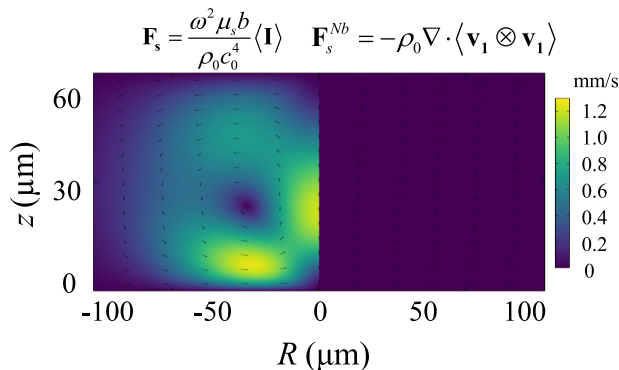


FIG. 4. The streaming simulation of two source terms at 1.5 GHz when the vibration velocity of the transducer surface is $U_{ac} = 0.1$ m/s. The radius of the transducer is $a = 50$ μm . The channel height is $L_c = 60$ μm and the width is 200 μm . The left half is simulated by using the recast source term [Eq. (7)], and the right half is simulated with Nyborg's source term [Eq. (9)]. The uniform colorbar is used. The color background represents the velocity distribution of the hydrodynamic flow and the arrows represent the flow directions. Significant differences between the two source terms are observed to calculate the streaming-induced velocities. The maximum flow velocity by Nyborg's expression is 0.02 mm/s, which is much smaller than that with the present source term in Eq. (7).

together for ease of comparison: the left half is for the source term in Eq. (7) while the right half is for the source term by Nyborg in Eq. (9). It is obvious that the streaming velocities of these two terms have a significant difference at this time. Note that the main differences lie in the magnitudes of the maximum flow velocities, while the hydrodynamic flow patterns are similar because of the conservation of fluid flow in the microchannels. Through this example, it is obvious that there are problems in using the classical source term by Nyborg for acoustic streaming simulation. In addition, it will be noteworthy that an empirical expression of the source term [1,3] is widely used for the present simulations of gigahertz streaming which is limited to the plane-wave case and could not predict the exact values of the hydrodynamic flow velocities.

IV. WEAKLY NONLINEAR PROPAGATION WITH HIGH-ORDER ACOUSTIC HARMONICS

The source term of the bulk streaming in Eq. (7) is proper under the assumption of linear acoustic propagation. However, it does not apply if nonlinear acoustics are considered (e.g., high-order harmonics) for the streaming phenomenon since the pressure field may include the contribution of multiple frequencies. To solve the issue, we rederive a general expression of the sole source term for acoustic streaming with the multifrequency acoustic field in terms of only acoustic pressure p_1 as follows [see Eq. (B3)]:

$$\mathbf{F}_s = \left(\frac{4}{3} \mu_s + \mu_b \right) \left\langle \frac{p_1}{c_0^4 \rho_0^2} \nabla \frac{\partial p_1}{\partial t} \right\rangle \quad (16)$$

with the detailed derivation of the source expression given in Appendix B 2. This formula has the advantage to compute the incompressible hydrodynamic fluid motion induced by acoustic streaming once the acoustic field can be calculated.

Recall the Goldberg number as first introduced in Sec. II, which plays an important role in the viscous process considering nonlinear effects [8]. It measures the relative importance of nonlinear effects and dissipation effects. Since only weakly nonlinear propagation is considered in this work and there are no shock waves as assumed, the following will derive the source terms with Goldberg numbers within $\Gamma \ll 1$ and $\Gamma \sim 1$ based on the analytical expressions of harmonic waves from a finite-amplitude Gaussian beam in a fluid by Du and Breazeale [24].

A. Acoustic pressure and frequency spectrum at different Γ

To calculate the acoustic streaming with nonlinear propagation, we need to solve the pressure field according to Eq. (16). The nonlinear propagation of acoustics could be calculated with either analytical methods or numerical simulations. This part will review the analytical expressions of the acoustic pressure fields of the fundamental and second-order harmonics by Du and Breazeale for a Gaussian beam from a piston transducer [24]. As Goldberg points out, the shock wave will not be formed when $\Gamma < 1$. This is because the dissipation effect is significant under the circumstance, and the harmonics cannot be effectively accumulated. For the piston transducer, we assume that the vibration velocity of the sound source satisfies the Gaussian function and take the Gaussian coefficient as a unit for simplicity:

$$U(R) = U_{ac} e^{-R^2/a^2}, \quad (17)$$

where R is the radial coordinate and a is the radius of the piston transducer. By taking the method from Du and Breazeale, we can expand its acoustic pressure waveform into Fourier series [see Eqs. (A1) and (A4) in Ref. [24]]:

$$p_1 = \sum_{n=1}^2 P_n \sin \left[n\omega \left(t - \frac{z}{c_0} \right) \right], \quad (18)$$

where P_n represents the spatial components of the n th harmonic acoustic pressure, t designates time, and z is the distance from the transducer surface in the propagation direction. This expression illustrates the physical mechanism of the nonlinear pressure field in terms of the addition of different orders of harmonics. For the fundamental component (the first order),

$$P_1(f | z) = p_{am} e^{-\alpha z} \exp(-R^2/a^2). \quad (19)$$

and for the second-order harmonics

$$P_2(f | z) = \frac{p_{am}^2 k \beta e^{-4\alpha z}}{4\alpha \rho_0 c_0^2} e^{(-2R^2/a^2)} (e^{2\alpha z} - 1), \quad (20)$$

where the pressure amplitude at the center of the transducer surface is $p_{am} = \rho_0 c_0 U_{ac}$ and $\alpha = 1/L_a$ is the attenuation coefficient. The detailed derivation is briefly organized in Appendix B 3.

An example shows that the nonlinear effect starts around $\Gamma = 3$ for a plane wave by Hamilton and Blackstock, while other scholars select 4.5 as the threshold for shock formation [9]. To compare the pressure fields with or without high-order harmonics, two pressure amplitudes are selected to make the Goldberg numbers $\Gamma = 0.1$ and $\Gamma = 1.8$ for the Gaussian beam, respectively. The radius of the piston transducer is $a = 50 \mu\text{m}$ with the excitation frequency $f = 1.5 \text{ GHz}$. The pressure fields along the propagation direction z are computed with the analytical method and numerical simulations based on COMSOL [25]. These two results agree well with each other and are shown (one blue curve for brevity) in Fig. 5(a) at $p_{am} = 0.6 \text{ MPa}$ and (c) at $p_{am} = 10 \text{ MPa}$. The attenuation distance L_a is indicated by the vertical dashed lines. To illustrate the nonlinear high-order harmonics when $\Gamma > 1$, the frequency spectrum based on fast Fourier transform is calculated as shown in Figs. 5(b) and 5(d). It could be observed that there is a sharp peak at $f = 3 \text{ GHz}$ for $\Gamma = 1.8$ in the frequency spectrum of Fig. 5(d) which comes from the contribution of the second-order harmonics.

B. Source terms of streaming with and without high-order harmonics

According to the general source term of acoustic streaming in Eq. (16), explicit expressions with and without high-order harmonics could be obtained once the pressure fields are known. For the situation with only the fundamental component, by the insertion of Eq. (18) with (19) into Eq. (16), we can rewrite the axial body force F_z^s as (note n is truncated up to 1 for the fundamental wave case)

$$F_z^s = \frac{\alpha}{\rho_0 c_0^2} |P_1|^2, \quad (21)$$

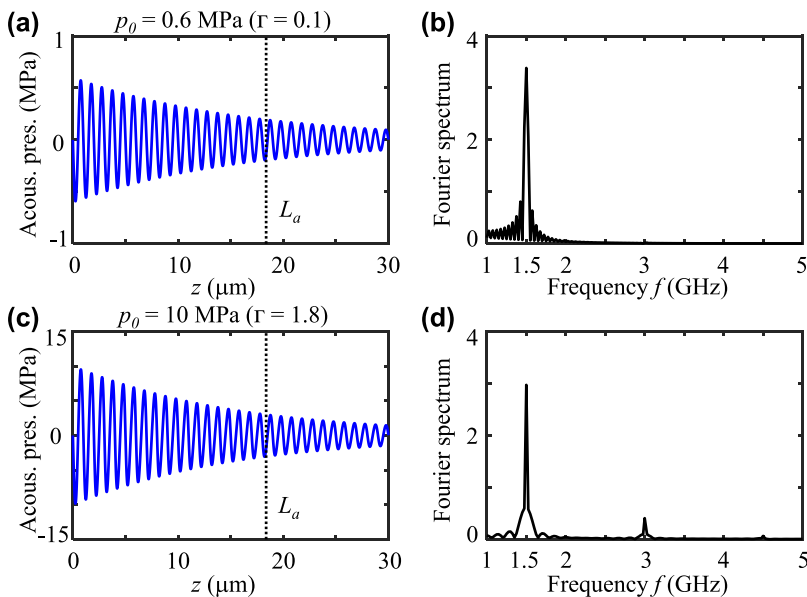


FIG. 5. Acoustic pressure based on the theoretical method in Ref. [24] and frequency spectrum with two different Goldberg numbers. (a) For $\Gamma = 0.1$, the pressure amplitude is $p_{\text{am}} = 0.6$ MPa with the attenuation distance $L_a = 18.4$ μm (indicated by the black dotted line) and the shock distance $L_s = 168.1$ μm . (b) Only the fundamental wave appears along with a few sidelobes. There are no obvious high-order harmonics in the frequency spectrum. (c) For $\Gamma = 1.8$, the pressure amplitude $p_{\text{am}} = 10$ MPa with $L_a = 18.4$ μm and $L_s = 10.1$ μm . (d) Different from the results in (b), the second-order harmonic wave appears in this case.

where $|P_1|^2 = p_{\text{am}}^2 e^{-2\alpha z} e^{-2R^2/a^2}$. Similarly, by substituting Eq. (18) into Eq. (16), the axial body force F_z^h considering the second-order harmonics can be expressed as

$$F_z^h = \frac{\alpha}{\rho_0 c_0^2} \sum_{n=1}^2 (n^2 |P_n|^2), \quad (22)$$

where the upper right “ h ” represents the body force with the contribution of the second-order harmonics. Indeed, this source term works for high-order harmonics when $n > 2$. When only the fundamental wave is considered ($n = 1$), Eq. (22) degenerates into (21). Note that the lateral component of the source term vanishes after the time-average procedures, i.e., $F_R = 0$ for the cases with and without high-order harmonics.

To study the contribution of the second-order harmonics on the total pressure field and body force, the same piston transducer is used with the initial pressure amplitude $p_{\text{am}} = 10$ MPa at the excitation frequency $f = 1.5$ GHz. The sizes of the microchannel are the same as those in Fig. 4. The simulation flowchart is given in Fig. 3(b) with the pressure field computed based on the theoretical method in MATLAB and the induced streaming obtained by using COMSOL. Note that the hydrodynamic flow speed can reach up to 1 m/s, leading to $\text{Re}_{\text{hd}} \gg 1$; the “laminar” interface is applied in this section. The normalized pressure fields versus the propagation distance z of the fundamental (red solid line) and second-order (blue dotted line) harmonic waves are shown in Fig. 6. The surface of the transducer is defined as $z = 0$. The amplitude of the fundamental component decreases versus z because of the wave absorption, while the pressure amplitude of the second-order harmonics increases from the transducer surface to a maximum value at $z \approx 6$ μm , which agrees with the fact that the nonlinearity effect is dominant over the dissipation close to the source. In addition, the relative axial body force with the consideration of the second-order harmonics with

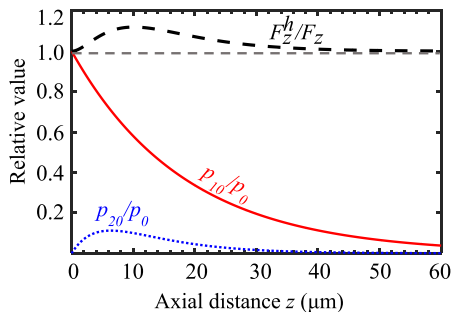


FIG. 6. The ratios of pressure magnitude of the fundamental wave p_{10}/p_{am} (red solid line), the second harmonic wave p_{20}/p_{am} (blue dotted line), and the body force F_z^h/F_z (black dashed line) change along the axial direction when the pressure magnitude is $p_{\text{am}} = 10$ MPa and the frequency is 1.5 GHz. F_z^h is the axial body force considering the contribution of both the fundamental and the second-order harmonics, which is defined by Eq. (22). F_z is the volume force considering only the fundamental frequency acoustic pressure, which is determined by Eq. (21). The fundamental sound pressure decreases with the increase of axial distance, and the second harmonic sound pressure and body force increase first and then reduce with the increase of axial distance. The attenuated energy of the fundamental wave turns into high-order harmonics.

respect to only the fundamental wave contribution is plotted versus z with the black dashed line in Fig. 6. A horizontal gray dashed line is also provided as a reference. It is shown that the excess of the body force comes from the contribution of the second-order harmonics.

To further explore the streaming-induced hydrodynamic motion in the microchannel, we take the same configuration as in Fig. 6 but double the pressure amplitude $p_{\text{ac}} = 20$ MPa to enhance the contribution of the second-order harmonics. The left half of Fig. 7 shows the streaming patterns with only the fundamental component, while the right half is for the situation with both the fundamental and second-order harmonics. The colormap in the background indicates the velocity amplitude of the hydrodynamic flows with the arrows giving the flow directions. The maximum hydrodynamic flow velocity increases more than 20% if the second harmonic component is taken into consideration, as shown in Fig. 7.

V. CONCLUSION AND DISCUSSION

The theory of the source term for bulk acoustic streaming has been developed with an emphasis on the nonlinear propagation in the frequency regime of gigahertz. A dimensionless number

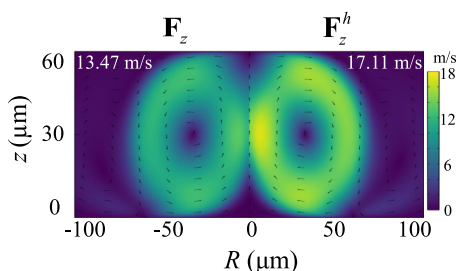


FIG. 7. Streaming results without and with the second-order harmonics at 1.5 GHz. The acoustic pressure is 20 MPa. The left half shows the acoustic streaming field with only the contribution of the fundamental wave with the maximum flow speed of 13.47 m/s, calculated by Eq. (21). The right half considers the contribution of the second-order harmonics with the maximum flow speed of 17.11 m/s, which is based on Eq. (22). The color depth represents the streaming velocity.

called the Goldberg number (Γ) is introduced to measure the importance of acoustic nonlinearity relative to dissipation at gigahertz. This work makes it possible to compute the streaming-induced microfluidic motion for the recent gigahertz devices in a better manner instead of using the empirical formulas [1,3]. As shown in the numerical simulation, the contribution of high-order harmonics could increase the maximum velocity of hydrodynamic flows up to 20% if only the fundamental component is considered in linear propagation. In addition, the source term of bulk streaming in linear acoustic propagation is revisited in the form of wave damping and acoustic intensity [17]. More importantly, we propose analytical and numerical examples to show the contradictory results by the source term of linear propagation and the classic expression by Nyborg [13,14]. The term by Nyborg should be avoided by others (e.g., see Ref. [26]) since it contains the contribution of acoustic radiation pressure [15,17].

The alternative method to compute the bulk streaming is the full-model direct numerical simulation (DNS) [7]. However, it will take more computational cost and will be challenging to handle the full simulation in the three-dimensional (3D) domain. The computational burden could be relieved with the effective boundary conditions developed by Bach and Bruus [27] and using the axial symmetry of the geometrical model [28]. However, attention should still be paid to the simulation of 3D bulk streaming if there is no axial symmetry with either the present theory or DNS; for instance, the drop-shaped transducer working at gigahertz in a microchannel [3]. It should be noted that this work could be helpful to design acoustical tweezers for particle trapping with the consideration of both the acoustic radiation pressure [29,30] and the streaming-induced drag force.

ACKNOWLEDGMENTS

Z.G. acknowledges support from the National Natural Science Foundation of China (24Z990200542), Shanghai Jiao Tong University for the startup funding (WH220401017, WH22040121), and the XIAOMI Foundation.

APPENDIX A: DERIVATION OF THE SOLE SOURCE OF ACOUSTIC STREAMING

1. First-order perturbation expansion

To derive the source term of acoustic streaming (i.e., sound-induced fluid motion), we need to bridge the acoustic field (acoustic pressure p_1 and hydrodynamic velocity \mathbf{v}_1) with the fluid velocity \mathbf{v}_2 . Using the perturbation method, we need to expand the fields up to the first-order and second-order terms. Firstly, we expand the fields up to the linear limit with the following perturbation:

$$\begin{aligned}\rho &= \rho_0 + \rho_1, \\ p &= p_0 + p_1, \\ \mathbf{v} &= \mathbf{0} + \mathbf{v}_1.\end{aligned}\tag{A1}$$

Substituting Eq. (A1) into Eqs. (2) and (3), we can obtain the first-order formulas of mass and momentum conservation, respectively:

$$\frac{\partial \rho_1}{\partial t} + \rho_0 \nabla \cdot \mathbf{v}_1 = 0,\tag{A2}$$

$$\rho_0 \frac{\partial \mathbf{v}_1}{\partial t} = -\nabla p_1 + \mu_s \Delta \mathbf{v}_1 + \left(\frac{\mu_s}{3} + \mu_b \right) \nabla \nabla \cdot \mathbf{v}_1,\tag{A3}$$

where $\Delta \mathbf{v}_1 = \nabla \cdot (\nabla \mathbf{v}_1)$. Since the first-order acoustic field is defined as irrotational (i.e., $\nabla \times \mathbf{v}_1 = 0$), Eq. (A3) can be further changed into the following form:

$$\rho_0 \frac{\partial \mathbf{v}_1}{\partial t} = -\nabla p_1 + \left(\frac{4}{3} \mu_s + \mu_b \right) \Delta \mathbf{v}_1.\tag{A4}$$

It should be noted that the derivation of the above equation uses the mathematical identity of the vector Laplacian: $\nabla \nabla \cdot \mathbf{v}_1 = \nabla^2 \mathbf{v}_1 + \nabla \times \nabla \times \mathbf{v}_1$ [see Eq. (3.70) in Ref. [31]].

2. Second-order perturbation expansion

Since acoustic streaming is a nonlinear phenomenon, we need to expand the fields up to the second order as given in Eq. (5). After substitution into the mass conservation equation, one obtains

$$\frac{\partial \rho_2}{\partial t} + \nabla \cdot (\rho_1 \mathbf{v}_1) + \rho_0 \nabla \cdot \mathbf{v}_2 = 0. \quad (\text{A5})$$

Considering the steady-state acoustic streaming:

$$\rho_0 \nabla \cdot \mathbf{v}_2 = -\nabla \cdot (\rho_1 \mathbf{v}_1), \quad (\text{A6})$$

where the mass source term $-\nabla \cdot (\rho_1 \mathbf{v}_1)$ at the right-hand side of the equation represents the compressibility. In theory, because the phase difference of the first-order velocity \mathbf{v}_1 and density ρ_1 is $\pi/2$, one has $\langle \rho_1 \mathbf{v}_1 \rangle = 0$ after performing the time averaging. In other words, the mass source term is zero and the assumption of incompressibility is reasonable. Throughout the whole work, the incompressible flow assumption is held, so that

$$\nabla \cdot \mathbf{v}_2 = 0. \quad (\text{A7})$$

Before expanding the momentum conservation equation [Eq. (3)] up to the second-order, we first use the mass conservation to cancel some items in the momentum conservation [see Eq. (3)]:

$$\left[\frac{\partial \rho}{\partial t} + \nabla \cdot (\rho \mathbf{v}) \right] \mathbf{v} + \rho \frac{\partial \mathbf{v}}{\partial t} + \rho \mathbf{v} \cdot \nabla \mathbf{v} = -\nabla p + \mu_s \Delta \mathbf{v} + \left(\frac{\mu_s}{3} + \mu_b \right) \nabla \nabla \cdot \mathbf{v} \quad (\text{A8})$$

with the terms in the first square brackets vanishing based on the global mass conservation as given in Eq. (2). Note that the identity $\nabla \cdot (\rho \mathbf{v} \otimes \mathbf{v}) = \rho \mathbf{v} \cdot \nabla (\mathbf{v}) + \mathbf{v} \nabla \cdot (\rho \mathbf{v})$ is used here. By insertion of Eq. (5) into (A8) and taking the equation up to the second order:

$$\rho_0 \frac{\partial \mathbf{v}_2}{\partial t} + \rho_1 \frac{\partial \mathbf{v}_1}{\partial t} + \rho_0 \mathbf{v}_1 \cdot \nabla \mathbf{v}_1 = -\nabla p_2 + \mu_s \Delta \mathbf{v}_2 + \left(\frac{\mu_s}{3} + \mu_b \right) \nabla \nabla \cdot \mathbf{v}_2. \quad (\text{A9})$$

Since only the steady acoustic streaming is of interest, the first term of Eq. (A9) vanishes with $\partial \mathbf{v}_2 / \partial t = 0$.

The last term on the right-hand side in the second-order momentum conservation equation [Eq. (A9)] vanishes. To isolate the hydrodynamic fluid motion from the acoustic perturbation over time (i.e., $\partial \mathbf{v}_1 / \partial t$), we need to recall the first-order momentum conservation in Eq. (A4), which is rewritten as the following for convenience:

$$\rho_1 \frac{\partial \mathbf{v}_1}{\partial t} = -\frac{\rho_1}{\rho_0} \nabla p_1 + \frac{\rho_1}{\rho_0} \left(\frac{4}{3} \mu_s + \mu_b \right) \Delta \mathbf{v}_1. \quad (\text{A10})$$

Substituting Eq. (A10) into Eq. (A9), we get

$$-\frac{\rho_1}{\rho_0} \nabla p_1 + \frac{\rho_1}{\rho_0} \left(\frac{4}{3} \mu_s + \mu_b \right) \Delta \mathbf{v}_1 + \rho_0 \mathbf{v}_1 \cdot \nabla \mathbf{v}_1 = -\nabla p_2 + \mu_s \Delta \mathbf{v}_2. \quad (\text{A11})$$

If we take the time average of the above Eq. (A11) and use the definitions of kinetic energy density $\langle \mathcal{K} \rangle = \langle \rho_0 \mathbf{v}_1 \cdot \nabla \mathbf{v}_1 \rangle = \langle \nabla (1/2 \rho_0 \mathbf{v}_1^2) \rangle$ and potential energy density $\langle \mathcal{U} \rangle = \langle \rho_1 / \rho_0 \nabla p_1 \rangle = \langle \nabla [p_1^2 / (2 \rho_0 c_0^2)] \rangle$ (note that the first-order equation of state is applied here), the second-order momentum conservation equation can be expressed as

$$\nabla \langle \mathcal{L} \rangle + \left(\frac{4\mu_s}{3} + \mu_b \right) \left\langle \frac{\rho_1}{\rho_0} \Delta \mathbf{v}_1 \right\rangle = \langle -\nabla p_2 + \mu_s \Delta \mathbf{v}_2 \rangle, \quad (\text{A12})$$

where the time-averaged acoustic Lagrangian is defined as $\langle \mathcal{L} \rangle = \langle \mathcal{K} - \mathcal{U} \rangle$. As noted, the acoustic Lagrangian is independent of the viscous effect and hence not affected by the wave attenuation, while the acoustic streaming is induced by the transfer of acoustic momentum to the viscous mode through wave attenuation. That is to say, the averaged acoustic Lagrangian $\langle \mathcal{L} \rangle$ is not related to the steady acoustic streaming and can be balanced with a hydrostatic pressure gradient, having $\nabla p_2^* = \nabla p_2 + \langle \mathcal{L} \rangle$ [15,17]. Hence, the second-order momentum conservation equation can be finally written as

$$-\nabla p_2^* + \mu_s \Delta \mathbf{v}_2 + \mathbf{F}_s = 0, \quad (\text{A13})$$

where the sole source for steady acoustic streaming is

$$\mathbf{F}_s = -\left(\frac{4\mu_s}{3} + \mu_b\right) \left\langle \frac{\rho_1}{\rho_0} \Delta \mathbf{v}_1 \right\rangle. \quad (\text{A14})$$

We use the hydrodynamic Reynolds number Re_{hd} to characterize the relative contribution of the inertia term $\rho_0(\mathbf{v}_2 \cdot \nabla)\mathbf{v}_2$ and the viscosity term $\mu_s \nabla^2 \mathbf{v}_2$ [15]:

$$\text{Re}_{\text{hd}} = \frac{\rho_0 v_2 d}{\mu_s}, \quad (\text{A15})$$

where v_2 is the characteristic streaming velocity of the system, d is the characteristic length of the system, and $d \sim 60 \mu\text{m}$. The hydrodynamic Reynolds number is equal to 1 when the streaming velocity is

$$v_{\text{cr}} = \frac{\mu_s}{\rho_0 d} = 16.7 \text{ mm/s}. \quad (\text{A16})$$

When $\text{Re}_{\text{hd}} \gg 1$ ($v_2 \gg v_{\text{cr}}$), the inertia term $\rho_0(\mathbf{v}_2 \cdot \nabla)\mathbf{v}_2$ is dominant; the inertia term cannot be ignored and we use the Lighthill theory to simulate the acoustic streaming. At this point, the governing equation becomes

$$\rho_0(\mathbf{v}_2 \cdot \nabla)\mathbf{v}_2 + \mu_s \Delta \mathbf{v}_2 - \nabla p_2 = \mathbf{F}_s^{Nb}. \quad (\text{A17})$$

When $\text{Re}_{\text{hd}} \ll 1$ ($v_2 \ll v_{\text{cr}}$), the viscosity term is dominant, the $\rho_0(\mathbf{v}_2 \cdot \nabla)\mathbf{v}_2$ will disappear, and the governing equation will be restored to (A13).

This makes it possible to use commercial software like COMSOL to solve the acoustic streaming problems with the source term induced by acoustic field.

APPENDIX B: EXPLICIT EXPRESSIONS OF SOURCE TERMS

1. Monochromatic fundamental wave

For most applications using the acoustic streaming effect, the acoustic wave is considered as a monochromatic wave with the linear wave equation for the velocity as

$$\frac{\partial^2 \mathbf{v}_1}{\partial t^2} - c_0^2 \Delta \mathbf{v}_1 = 0, \quad (\text{B1})$$

where $\partial^2/\partial t^2 = -\omega^2$ for a single-frequency fundamental harmonic wave with $\omega = 2\pi f$ the angular frequency. Hence, the wave equation can be simplified as $\Delta \mathbf{v}_1 = -\omega^2 \mathbf{v}_1/c_0^2$. With insertion of the steady wave equation into the source term of Eq. (A14) with the combination of the first-order equation of state, the sole source of acoustic streaming is

$$\mathbf{F}_s = \left(\frac{4\mu_s}{3} + \mu_b\right) \frac{\omega^2}{c_0^4 \rho_0} \langle p_1 \mathbf{v}_1 \rangle \quad (\text{B2})$$

with the average acoustic density $\langle \mathbf{I} \rangle = \langle p_1 \mathbf{v}_1 \rangle$. This formula is also given in Eq. (19) of Ref. [16].

2. High-order harmonic waves

When the weak nonlinear effect induces a few high-order harmonics, e.g., up to the order of $n = 2$, the source term for the acoustic streaming given in Eq. (B2) will not apply, which is limited to the case of a single-frequency fundamental wave. Under this condition, we have to rederive the source term based on the general expression of Eq. (A14) with only two assumptions: the irrotational acoustic field ($\nabla \times \mathbf{v}_1 = 0$) and the incompressible streaming fluid field ($\nabla \cdot \mathbf{v}_2 = 0$). By combining the first-order mass conservation equation [see Eq. (A2)] and the first-order equation of state, the relation between the acoustic pressure p_1 and the velocity vector \mathbf{v}_1 can be derived as $\nabla p_1 / (\rho_0 c_0^2) = \Delta \mathbf{v}_1$ with vector identity $\nabla \nabla \cdot \mathbf{v}_1 = \nabla^2 \mathbf{v}_1 + \nabla \times \nabla \times \mathbf{v}_1$. By insertion of this relation into the general expression of body force \mathbf{F}_s in Eq. (A14), one can derive the following source form including only the acoustic pressure:

$$\mathbf{F}_s = \left(\frac{4}{3} \mu_s + \mu_b \right) \left\langle \frac{p_1}{c_0^4 \rho_0^2} \nabla \frac{\partial p_1}{\partial t} \right\rangle. \quad (\text{B3})$$

This form is helpful to deal with acoustic streaming problems if the acoustic field with high-order harmonics is solved with either analytical or numerical methods.

Consider the acoustic pressure form including low-order harmonics [24]:

$$p_1 = P_1 \sin \left[\omega \left(t - \frac{z}{c_0} \right) \right] + P_2 \sin \left[2\omega \left(t - \frac{z}{c_0} \right) \right] = \sum_{n=1}^2 P_n \sin \left[n\omega \left(t - \frac{z}{c_0} \right) \right]. \quad (\text{B4})$$

Substituting the above equation into Eq. (B3), the following form of body force can be obtained:

$$F_z^h = \frac{\alpha}{\rho_0 c_0^2} \sum_{n=1}^2 \langle n^2 P_n^2 \rangle. \quad (\text{B5})$$

The orthogonality of trigonometric functions is used in the derivation of the above formula, that is, $1/T \int_0^T [\sin(n\omega t) \sin(m\omega t)] dt = 0$ when $n \neq m$ and $T = 2\pi/\omega$ is the period for the fundamental harmonics.

3. Pressure fields of high-order harmonic waves by Du and Breazeale

By using the perturbation method to solve the nonlinear wave equation (first proposed by Kuznetsov [32]), we can obtain the following fundamental quasilinear solution [see Eq. (4) in Ref. [24] with $z/z_0 \ll 1$ and $\gamma \approx \pi/2$]:

$$P_1(f | z) = p_{\text{am}} \frac{e^{-\alpha z}}{\sqrt{1 + (z/z_0)^2}} \exp \left(-\frac{R^2/a^2}{1 + (z/z_0)^2} \right), \quad (\text{B6})$$

where $z_0 = ka^2/2$. It is noted that the near-field condition is applicable ($z \ll z_0$) when the channel height is small. In this case, the diffraction effect is very weak, and therefore the acoustic pressure in Eq. (B6) can be simplified as

$$P_1(f | z) = p_{\text{am}} e^{-\alpha z} e^{(-R^2/a^2)}. \quad (\text{B7})$$

Note that in Blackstock's study [8], the extra attenuation (EXDB) is very small (the EXDB refers to the loss beyond the normal small signal attenuation $e^{-\alpha z}$) when the Goldberg number $\Gamma \sim 1$. Under this condition, low-order harmonics will be generated, while no shock waves will be formed. With the help of the Hankel transform, P_2 can be calculated by following the work of Du and Breazeale [see Eqs. (11) and (12) in Ref. [24]]:

$$P_2(f | z) = \frac{p_{\text{am}} D_0 e^{-4\alpha z}}{4\sqrt{1 + (z/z_0)^2}} \exp \left(-\frac{2R^2/a^2}{1 + (z/z_0)^2} \right) \sqrt{H_2^2 + F_2^2} \quad (\text{B8})$$

with

$$H_2 = \int_0^\sigma \frac{e^{2\alpha z_0 \sigma'}}{\sqrt{1 + (z/z_0)^2}} \cos[\tan^{-1}(\sigma')] d\sigma' \quad (\text{B9})$$

and

$$F_2 = \int_0^\sigma \frac{e^{2\alpha z_0 \sigma'}}{\sqrt{1 + (z/z_0)^2}} \sin[\tan^{-1}(\sigma')] d\sigma', \quad (\text{B10})$$

where $\sigma = z/z_0$ and $D_0 = 2z_0/L_s$. Considering the near-field condition $z \ll z_0$, we can further simplify the second harmonic acoustic pressure Eq. (B8) as

$$P_2(f | z) = \frac{P_{\text{am}}^2 k \beta e^{-4\alpha z}}{4\alpha \rho_0 c_0^2} \exp(-2R^2/a^2)(e^{2\alpha z} - 1). \quad (\text{B11})$$

Note that the solutions for higher harmonics up to the fourth order are also listed in the Appendix of Ref. [24].

-
- [1] W. Cui, H. Zhang, H. Zhang, Y. Yang, M. He, H. Qu, W. Pang, D. Zhang, and X. Duan, Localized ultrahigh frequency acoustic fields induced micro-vortices for submilliseconds microfluidic mixing, *Appl. Phys. Lett.* **109**, 253503 (2016).
- [2] W. Cui, L. Mu, X. Duan, W. Pang, and M. A. Reed, Trapping of sub-100 nm nanoparticles using gigahertz acoustofluidic tweezers for biosensing applications, *Nanoscale* **11**, 14625 (2019).
- [3] Y. Yang, L. Zhang, K. Jin, M. He, W. Wei, X. Chen, Q. Yang, Y. Wang, W. Pang, X. Ren, and X. Duan, Self-adaptive virtual microchannel for continuous enrichment and separation of nanoparticles, *Sci. Adv.* **8**, eabn8440 (2022).
- [4] R. J. Shilton, M. Travaglini, F. Beltram, and M. Cecchini, Nanoliter-droplet acoustic streaming via ultra high frequency surface acoustic waves, *Adv. Mater.* **26**, 4941 (2014).
- [5] M. B. Dentry, L. Y. Yeo, and J. R. Friend, Frequency effects on the scale and behavior of acoustic streaming, *Phys. Rev. E* **89**, 013203 (2014).
- [6] W. Cui, W. Pang, Y. Yang, T. Li, and X. Duan, Theoretical and experimental characterizations of gigahertz acoustic streaming in microscale fluids, *Nanotechnol. Precis. Eng.* **2**, 15 (2019).
- [7] A. G. Steckel, Theory and modeling of thin-film actuation in microscale acoustofluidics, Ph.D. dissertation, Technical University of Denmark, Kongens Lyngby, Denmark, 2021.
- [8] D. T. Blackstock, Thermoviscous attenuation of plane, periodic, finite-amplitude sound waves, *J. Acoust. Soc. Am.* **36**, 534 (1964).
- [9] M. F. Hamilton, Effective Gol'dberg number for diverging waves, *J. Acoust. Soc. Am.* **140**, 4419 (2016).
- [10] R. M. White and F. W. Voltmer, Direct piezoelectric coupling to surface elastic waves, *Appl. Phys. Lett.* **7**, 314 (1965).
- [11] H. Zhang, W. Pang, H. Yu, and E. S. Kim, High-tone bulk acoustic resonators on sapphire, crystal quartz, fused silica, and silicon substrates, *J. Appl. Phys.* **99**, 124911 (2006).
- [12] C. Eckart, Vortices and streams caused by sound waves, *Phys. Rev.* **73**, 68 (1948).
- [13] W. L. Nyborg, Acoustic streaming due to attenuated plane waves, *J. Acoust. Soc. Am.* **25**, 68 (1953).
- [14] W. L. Nyborg, *Acoustic Streaming in Physical Acoustics* (Academic, New York, 1965), Vol. 2, pp. 265–331.
- [15] J. Lighthill, Acoustic streaming, *J. Sound Vib.* **61**, 391 (1978).
- [16] M. Baudoin and J.-L. Thomas, Acoustic tweezers for particle and fluid micromanipulation, *Annu. Rev. Fluid Mech.* **52**, 205 (2020).

- [17] A. Riaud, M. Baudoin, O. B. Matar, J.-L. Thomas, and P. Brunet, On the influence of viscosity and caustics on acoustic streaming in sessile droplets: An experimental and a numerical study with a cost-effective method, *J. Fluid Mech.* **821**, 384 (2017).
- [18] A. Panfilova, R. J. van Sloun, H. Wijkstra, O. A. Sapozhnikov, and M. Mischi, A review on B/A measurement methods with a clinical perspective, *J. Acoust. Soc. Am.* **149**, 2200 (2021).
- [19] COMSOL multiphysics 6.0, <http://cn.comsol.com/>.
- [20] J. Vanneste and O. Bühler, Streaming by leaky surface acoustic waves, *Proc. R. Soc. A* **467**, 1779 (2011).
- [21] P. B. Müller, R. Barnkob, M. J. H. Jensen, and H. Bruus, A numerical study of microparticle acoustophoresis driven by acoustic radiation forces and streaming-induced drag forces, *Lab Chip* **12**, 4617 (2012).
- [22] Z. Ni, C. Yin, G. Xu, L. Xie, J. Huang, S. Liu, J. Tu, X. Guo, and D. Zhang, Modelling of SAW-PDMS acoustofluidics: Physical fields and particle motions influenced by different descriptions of the PDMS domain, *Lab Chip* **19**, 2728 (2019).
- [23] N. Nama, R. Barnkob, Z. Mao, C. J. Kähler, F. Costanzo, and T. J. Huang, Numerical study of acoustophoretic motion of particles in a PDMS microchannel driven by surface acoustic waves, *Lab Chip* **15**, 2700 (2015).
- [24] G. Du and M. A. Breazeale, Harmonic distortion of a finite amplitude Gaussian beam in a fluid, *J. Acoust. Soc. Am.* **80**, 212 (1986).
- [25] COMSOL Multiphysics Model Library, Nonlinear Acoustics-Modeling of the 1D Westervelt Equation, 2013.
- [26] J. Eisener, A. Lippert, T. Nowak, C. Cairós, F. Reuter, and R. Mettin, Characterization of acoustic streaming beyond 100 MHz, *Phys. Procedia* **70**, 151 (2015).
- [27] J. S. Bach and H. Bruus, Theory of pressure acoustics with viscous boundary layers and streaming in curved elastic cavities, *J. Acoust. Soc. Am.* **144**, 766 (2018).
- [28] J. H. Jorgensen, Theory and modeling of thermoviscous acoustofluidics, Ph.D. dissertation, Technical University of Denmark, Kongens Lyngby, Denmark, 2022.
- [29] G. T. Silva, An expression for the radiation force exerted by an acoustic beam with arbitrary wavefront (I), *J. Acoust. Soc. Am.* **130**, 3541 (2011).
- [30] Z. Gong and M. Baudoin, Equivalence between angular spectrum-based and multipole expansion-based formulas of the acoustic radiation force and torque, *J. Acoust. Soc. Am.* **149**, 3469 (2021).
- [31] G. B. Arfken, H. J. Weber, and F. E. Harris, *Mathematical Methods for Physicists*, 7th ed. (Academic, New York, 2013), pp. 155 and 756–765.
- [32] V. P. Kuznetsov, Equations of nonlinear acoustics, *Sov. Phys. Acoust.* **16**, 467 (1971).